GENERAL ELECTRIC GLOBAL RESEARCH CENTER

UNIVERSITY OF TWENTE.

TURBOPROP ENGINE - COMPRESSOR TEST RIG

MSc. Internship report

STEPHAN EUVING

5/30/2016

PREFACE

From 01/03/2016 until 06/06/2016 I have performed an internship at General Electric located in Munich as a mandatory part of the master curriculum. At the Turbomachinery Aerodynamics Laboratory, I helped with the design of a test rig. Next year tests are to be performed with a compressor for a new turboprop engine.

INTERNSHIP LOCATION:

GE Global Research

General Electric Deutschland Holding GmbH
Freisinger Landstr. 50
85748 Garching b. München

INTERNSHIP SUPERVISORS:

Ir. R. Pannekeet and Dipl.-Ing. P. Schuler

GE Global Research
Freisinger Landstr. 50
85748 Garching b. München

UNIVERSITY SUPERVISOR:

Prof. dr. ir. H.W.M. Hoeijmakers

University of Twente
Drienerlolaan 5
7522 NB Enschede

SUMMARY

General Electric is one of the largest companies in the world and has shares in a large variety of businesses such as electronics, energy, aviation and healthcare. Within GE, the global research division (GE-GRC) is fully focused on research and development with several locations all over the world. During the internship at GE-GRC Munich I worked on a project within the Turbomachinery Aero Laboratory on a project for GE aviation.

General Electric has launched a European project making a turboprop for small airplanes. This GE engine will be the first engine designed, tested and manufactured in Europe. The turboprop is designed for small private airplanes such as the aircrafts produced by the American manufacturer Cessna. An engine used in the aviation industry has to be tested extensively before bringing it on the market. In 2017 the compressor of the engine will be tested in Munich. A project is running regarding these tests to get the test rig ready.

During the internship I helped in several tasks of this project. The first part I worked on was the inlet design of the test rig. A uniform flow has to enter the compressor in order to guarantee the correct inlet conditions to the compressor. Due to disturbances upstream of the compressor we ran CFD simulations in order to see if the inlet system allowed uniform flow at the inlet of the compressor. The CFD simulations have been done for two different configurations. The biggest difference between these configurations is the number of 90 ° bends upstream of the inlet. The introduction of swirl by 90° bends in the flow is analyzed. It is confirmed by the simulations that the extra 90 ° bend introduces extra swirl and rotation of the upstream valve does not change anything on the amount of swirl. Therefore, uniform fully developed flow is not guaranteed upstream the compressor. Inclusion of a flow straightener and the reduction of bends is the best way to ensure uniform flow at the compressor inlet.

A second task of the project concerned the design of the secondary air system. The design included the choice of measuring devices, which should allow the control of the flow. These measuring devices do not concern the primary airflow, i.e. the air for the propulsion, but the secondary air system. This air system supplies air for sealing, cooling and thrust balancing. Part of this air is supplied by primary air bleeds and a part has to be supplied from an external source. To be able to supply the right amount of gas, the mass-flow has to be measured. Given the required pressure, mass flow and temperature, the right measuring devices are chosen. The selection of these devices is based on temperature and pressure limits, turndown ratio, required pipe length and price. Other components discussed in this report are: valves, heat exchanger and the pipe diameters. In the end a drawing is made of the secondary air system with all components included.

CONTENTS

INTRODUCTION TO INTERNSHIP

Before the different tasks are discussed in next chapter, a short introduction to General Electric and the Global Research centers is needed to create the right perspective, necessary to understand how project are done within GE.

GE has several Global Research Centers all around the world. Currently 200 employees are located in the GE-GRC in Munich, the research center of Europe. As GE calls it a hub of commercial and industrial science and technology innovation, it is active in nearly all GE research fields. Within the Turbomachinery Aero Laboratory engineers deal with different kinds of turbomachinery of different business fields, such as aviation. An important part of this is the testing of the engine parts. The testing is done in a building of the Technical University of Munich. As GE is located at the university campus, the laboratory has a strong collaboration with TUM.

The Research Center is divided into several laboratories with their own specialization in industry. The Turbomachinery Aero Lab, with 14 full employees, is part of the Aero-Thermal & Mechanical Systems Europe together with three other laboratories at the Munich site. Some laboratories have a working student, intern, or graduation student working on smaller projects. All students have their desk in a student rooms where we had the opportunity to discuss problems and difficulties. This causes a dynamic and pleasant atmosphere and a possibility to exchange knowledge and experience.

During the internship, a direct supervisor was assigned with whom I had almost daily contact. I attended a weekly facility meeting to get a feeling of the internal developments of the project. Although most of the topics did not concern my direct tasks, it was very useful to follow the discussions. Because the project is at the design phase, it led to a very rapid developing and changing assignment where I experienced the challenges of R&D a little bit.

LIST OF SYMBOLS

Symbol		Units
R	Specific Gas constant	$\frac{J}{kgK}$
P	Pressure	Pa
T	Temperature	K
M	Mach Number	-
$\boldsymbol{\gamma}$	Specific heat ratio	-
$\boldsymbol{c_p}$	Specific heat at constant pressure	$\frac{J}{kgK}$
$\boldsymbol{\rho}$	Density	$\frac{kg}{m^3}$
U	Velocity	$\frac{m}{s}$
d	Diameter	m
A	Surface area	m^2
$\boldsymbol{\dot{m}}$	Mass flow	$\frac{kg}{s}$
$\boldsymbol{\mu}$	Dynamic viscosity	$\frac{kg}{m\,s}$
$\boldsymbol{\dot{V}}$	Volume flow	$\frac{m^3}{s}$
f	Friction factor	-
$\boldsymbol{\zeta}$	Pressure Drop coefficient	-

PROJECTS

General Electric has launched a European project making a turboprop for small aircrafts. In an article they stated: ''Textron Aviation, the world's largest maker of business propeller planes like Beechcraft Bonanza, Baron and King Air, said today it would use a brand new advanced turboprop engine developed by GE to power its latest single-engine turboprop plane. The engine burns 20 percent less fuel and produces 10 percent more power, compared to engines in its class'' (1). This GE engine will be the first engine designed, tested and manufactured in Europe. The tests of the compressor of this engine will be performed in the test facility in Munich. The tests will start at the beginning of 2017 and the test rig has now to be designed and build.

PROJECT 1: INLET CFD SIMULATIONS

Air is to be supplied from the facility to the compressor through a special designed inlet with a piping system attached. The piping design, schematically shown in Figure 1, shows a valve with a pipe mounted downstream, to provide fully developed flow at the inlet of the compressor. Flow profile distortion and swirl are the consequence of disturbances upstream, which in this case are the valve and bend. A general rule of thumb states that after 10-15 valve diameters the influence of these disturbances is gone and the flow is again fully developed (2). Serial disturbances will further increase this required length.

TASK DESCRIPTION:

Analysis of flow behavior at the compressor inlet due to disturbances upstream, using CFD simulations

There is limited space available in the facility. It is critical that, without having to extend the pipe between the valve and the inlet, the influence of the disturbances is gone. To investigate if the flow is indeed fully developed after 10-15 diameters and to find the amount of introduced swirl, CFD simulations are performed.

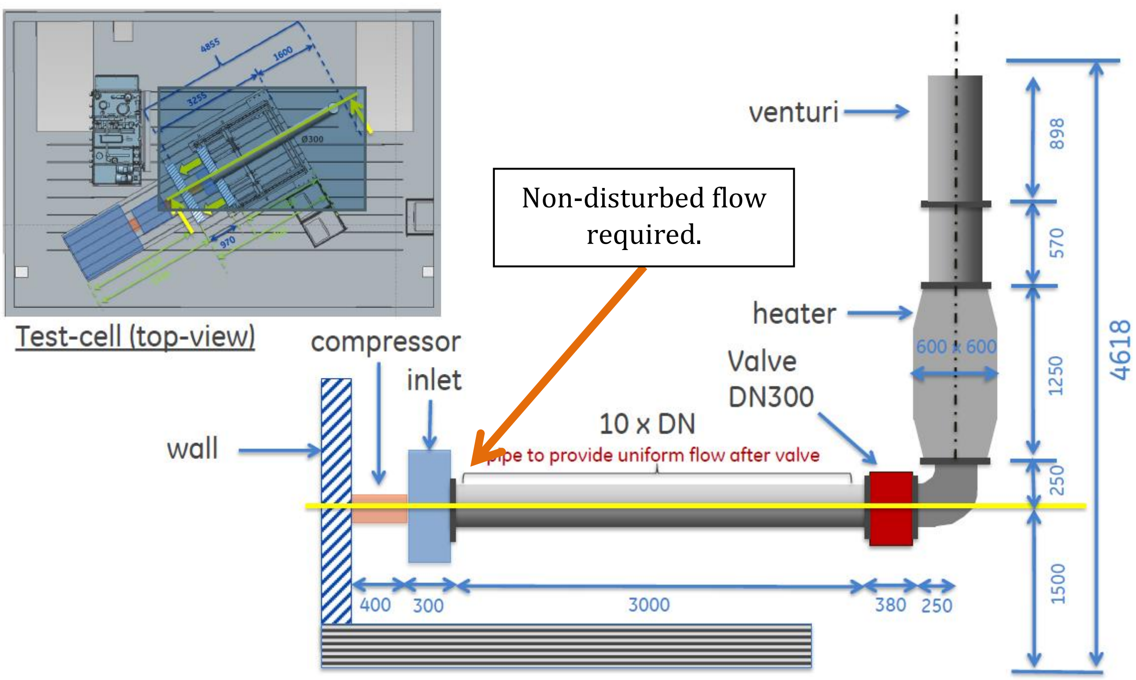

FIGURE 1: SCHEMATIC INLET PIPING DESIGN (LENGHTS IN MM)

In the schematic overview of Figure 1, air is supplied from the test facility itself. You could identify several minor disadvantages at this orientation of the inlet. If the test is running, the facility will heat up. Since there is only a heater installed, we are not able to cool the air down. It would be an advantage to supply cold air from outside the test facility to be able to control the temperature better. At the same time the heater weighs almost 200 kg. Supporting the heater in the upward orientation could be difficult.

One could think of changing the geometry to another orientation. If one would support the heavy heater at the floor and the air is supplied from the basement, which is not heated during the process, the design could look like Figure 2. The top view shows the position of the valve after a double 90-degree bend with a heater mounted in between. Another advantage compared to the other orientation would be easy opening of the rig, with easy access to the parts.

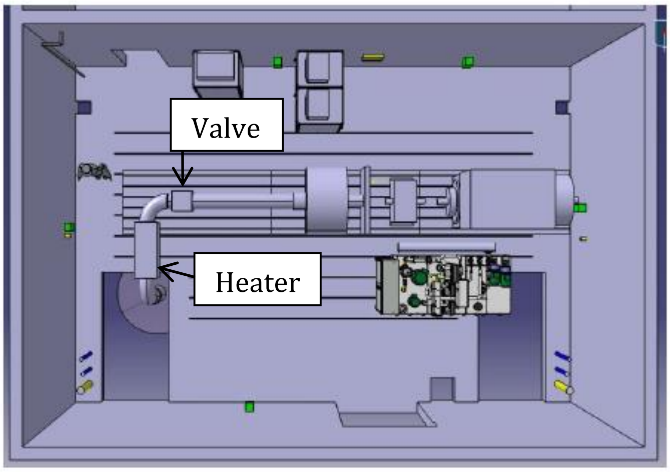

FIGURE 2: TOP VIEW LAB

A great concern would be the introduction of extra swirl due to the double 90 degrees bend and the re-arrangement of the test facility requires a lot of extra work.

To see which orientation would be preferred, both orientations will be discussed in the next section. A comparison between the flow behaviors is made company axial velocity, the angle of the flow at outlet and the streamlines of the flow.

SOFTWARE

For the CFD simulations several different software packages are used. Although I have encountered most of the programs while attending courses at the university, it was all in all a bit rusty. Since there was time for some tutorials, I took the advantage to improve my skills on the software described below. The software packages used for doing the simulations were:

- SolidWorks for 3D CAD models as input for the meshing program
- ICEM CFD for meshing
- ANSYS CFX for CFD calculations and analysis

MESHING

A disturbed flow profile will be introduced by the geometry. The valve will create non uniform turbulent and recirculating areas, while the bend will probably cause extra swirl to the flow. A quick look at the Reynolds number gives us an idea what the fully developed flow profile should look like. The DN 300 pipe with 3 kilograms of ambient air flowing through per second gives:

$$Re = \frac{\rho U d}{\mu} = \frac{\frac{\dot{m}}{\dot{V}} U d}{\mu} = \frac{\frac{\dot{m}}{AU} U d}{\mu} = \frac{\left(\frac{\dot{m}}{A}\right) d}{\mu} = \mathcal{O}(10^5)$$

For an internal pipe flow, the transition from laminar to turbulent typically occurs with the Reynolds number in the range of 2500. Since the Reynolds number is much higher the flow profile will turbulent and preferably fully developed. This has direct consequence for the CFD simulations. To be able to solve the Reynolds averaged Navier-Stokes equations, the problem needs to be closed, i.e. the introduction of a turbulence model. Complex areas have to be meshed correctly while paying attention to the boundary layer in the meanwhile.

The geometry of the valve is simplified, but even with a simplified geometry the disturbance will be created. A half-moon shape with thickness 100mm has been inserted in the valve as if the valve is half closed as shown in Figure 3.

FIGURE 3: VALVE AND SIMPLIFIED VALVE

After creating the geometry, ICEM is used to block the parasolid geometry to mesh the inlet piping. Since we are interested in the flow domain, the geometry is created as if it was the fluid domain. Heat transfer in the walls is neglected, so this is left out of the simulation. Figure 4 shows the fluid domain with the blocked geometry describing this fluid domain.

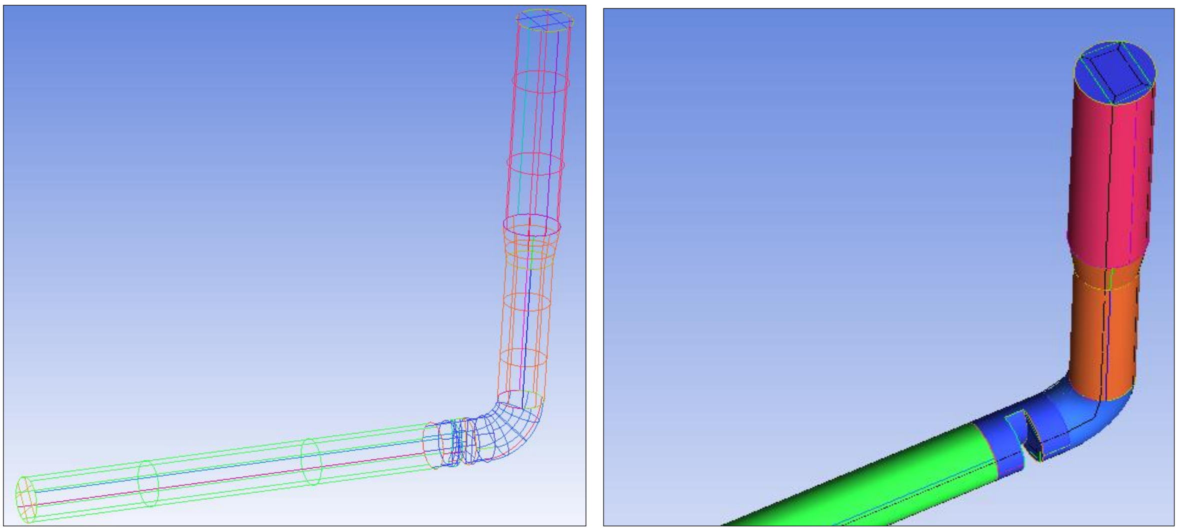

FIGURE 4: BLOCKED GEOMETRY

Due to the circular cross-sections, an O-grid is created to improve the quality of the meshed parts. After blocking the geometry, associating the right blocks to the geometry, creating the O-grid in these blocks and improving the position of the blocks, the geometry is ready for meshing.

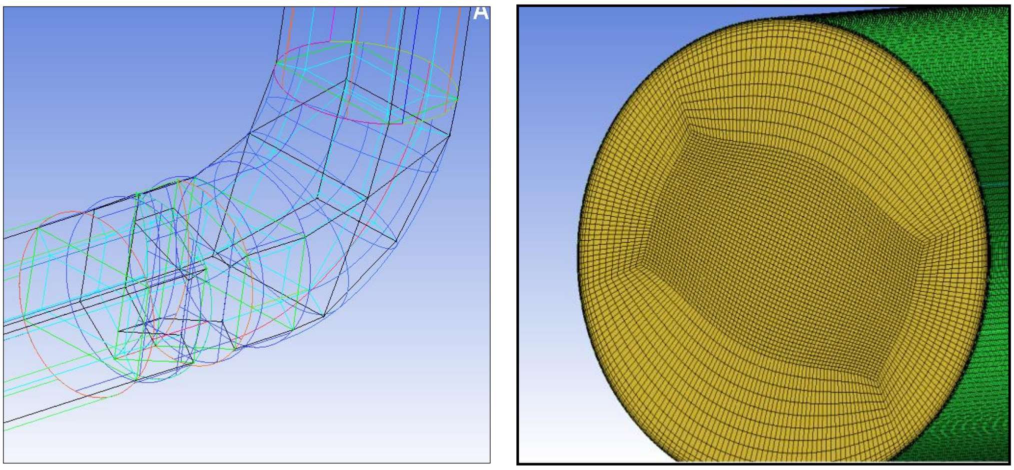

FIGURE 5: BLOCKED GEOMETRY WITH O-BLOCKS

The chosen turbulence model describes the local turbulent behavior, highly determines if the mesh is fine enough at the walls. In general, the boundary layer of turbulent flow consists out of three parts.

1. Wall layer: viscous shear dominated layer
2. Outer layer: inertial forces dominate the flow
3. Overlap layer

It depends on the turbulence model how many points of the mesh need to be in the laminar sub layer or the logarithmic region. In this case we chose to work with a SST turbulence model because of the following reasons (3):

- The SST model is a Low-Re turbulent model, i.e. able to describe the wall layer if there are sufficient points in this area.
- Even if we use a coarser grid at the boundary, a ω-based and SST model will be able to do automatic wall treatment, so is able to resorting to a wall function.

The SST model uses a combination of the k-omega and k-epsilon models and thus can be seen as a compromise between specialized models to establish a more general applicable model. This will give us more robust behavior.

QUALITY CONTROL

After a solid base for a mesh has been created, we can mesh using a bi-geometric distribution and the following parameters:

- First cell size: 0.1 mm
- Maximum cell size: 5 mm
- Max aspect ratio 1.5

A high quality mesh will ease the convergence to the discrete solution. Quality can be interpreted in many ways but in general the angles in the cells should not be too large/too small and the lengths of the cell sides should be in the same order of magnitude. An ideal Hexa element would be a perfect cube. Before processing the results, the quality is checked on defects, such as described above. Figure 6 and Figure 7 show two of the many parameters to check the quality.

2x2x2 determinant: The graph shows the calculation of the ratio of the smallest determinant of the Jacobian matrix divided by the largest determinant of the Jacobian matrix. This, in more general terms, is related to the aspect ratio of the elements. It shows the deviation from a perfect shaped element. A determinant value of 1 would indicate a perfectly regular mesh element, 0 would indicate an element degenerate in one or more edges, and negative values would indicate inverted elements. The figure shown is for a simulation with 12 million grid points and the parameters described above. (4)

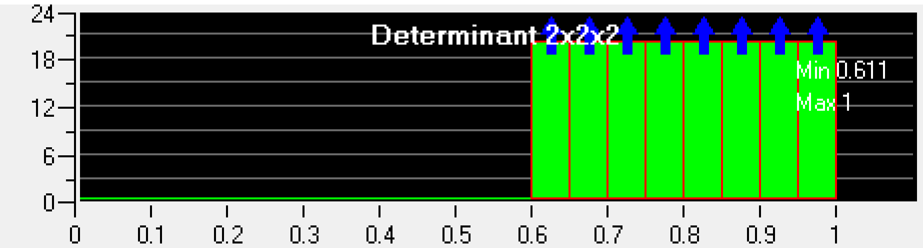

FIGURE 6: 2X2X2 DETERMINANT MESH

Quality: The Quality analysis uses weighted parameters which includes several aspects of the grid cell. It is a weighted diagnostic between the determinant, the maximal orthogonality and the maximum warpage. In the same way as with the 2x2x2 determinant a normalized value between -1 and 1 is given to the cell to quantify the quality. The minimum of the 3 normalized diagnostics will be used in the Quality parameter. In the result the leading parameter cannot be distinguished which is why literature advices to analyze the three parameters separately. But for a quick quality check this should be sufficient for now. (4)

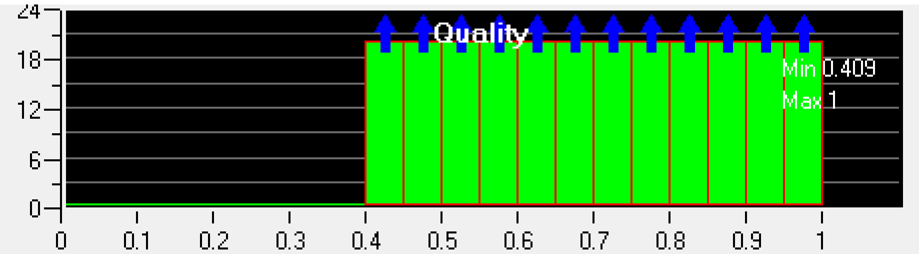

FIGURE 7: QUALITY MESH

FLOW RESULTS

In previous sections effort is put into ensuring a valid solution and the results can now be analyzed. For convergence the root mean square error is used. Figure 8 shows plots of the RMS residuals in the solved equations for the configuration with one 90-degree bend. The residual can be seen on the vertical axis. As can be seen convergence is established with a RMS residual in the order of 10^{-5}. Same convergence behavior can be seen for the configuration with two 90-degree bends. Let's have a look how the two geometries differ in result.

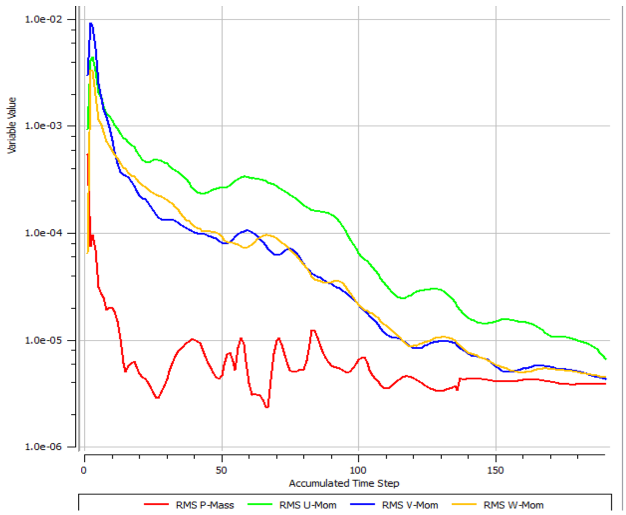

FIGURE 8: CONVERGENCE BAHAVIOUR CFD SIMULATION

VELOCITY STREAMLINES

The general flow behavior can be visualized by the streamlines of the flow. Both results can be found in Figure 9. A clear recirculation area behind the valve can be seen and it seems that the streamlines are not fully in axial direction, i.e. swirl is introduced. It would be good to know if the extra 90-degree bend introduces extra swirl in comparison to the configuration with only one bend.

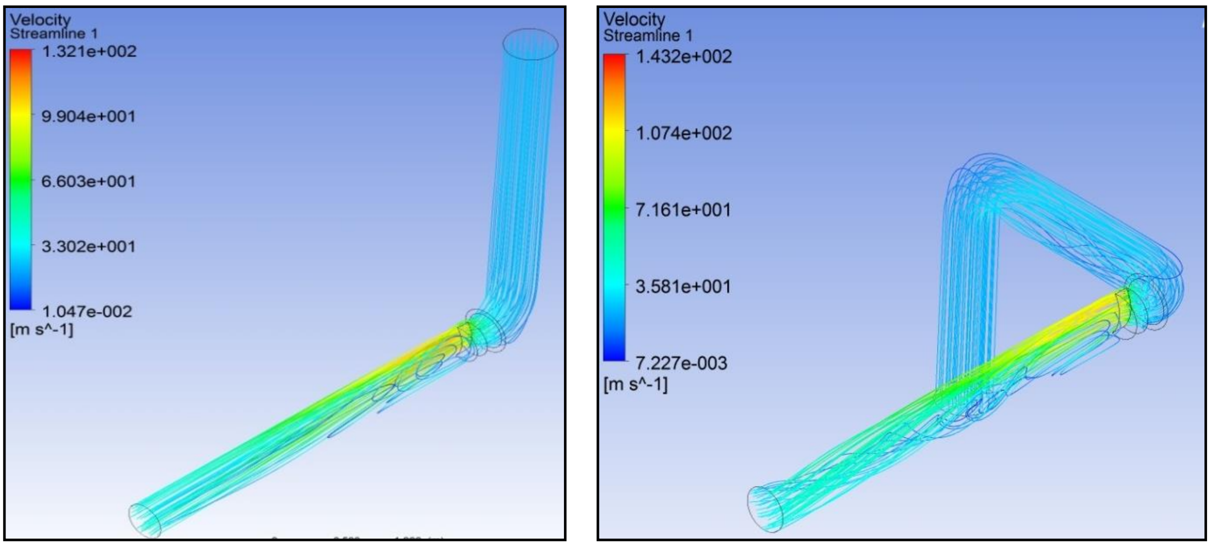

FIGURE 9: STREAMLINES IN THE TWO GEOMETRIES

To have a better look at the swirl effect we should have a look at a cross-section of the pipe at the outlet. The axial velocity contour plot at the cross section, Figure 10, shows similar velocities for both situation as expected. But there is a difference in distribution, likely due to the swirl effect.

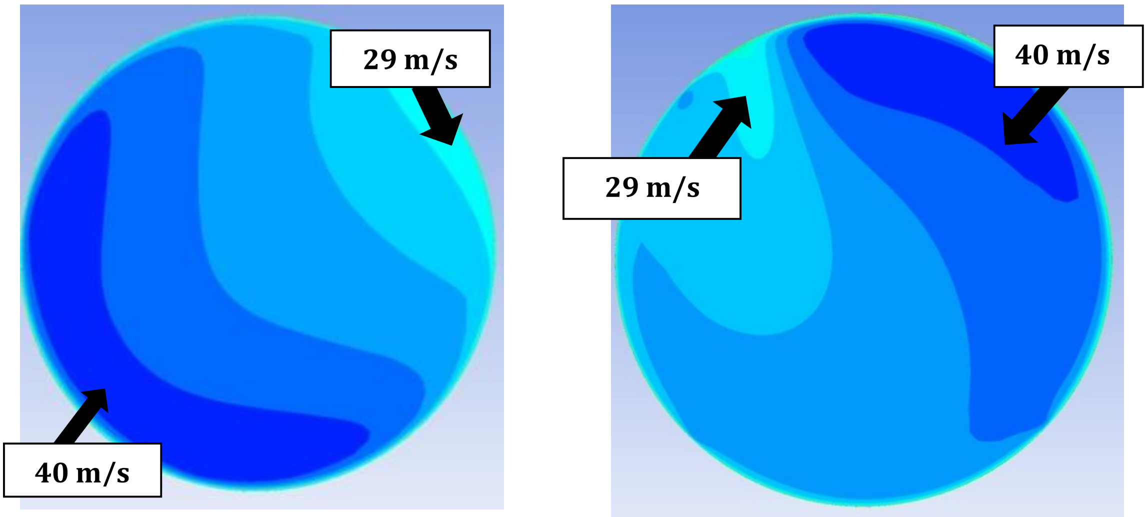

FIGURE 10: AXIAL FLOW (LEFT: CEILING CONFIG. /RIGHT: BASEMENT CONFIG.)

The axial velocity will be important when considering the flow profile at outlet but for now the magnitude of the velocities tangential to the surface are of greater interest. Since a Cartesian coordinate system is used and the x-axis is pointed in axial direction of the outlet pipe the outlet plane is mapped by the other two axes.

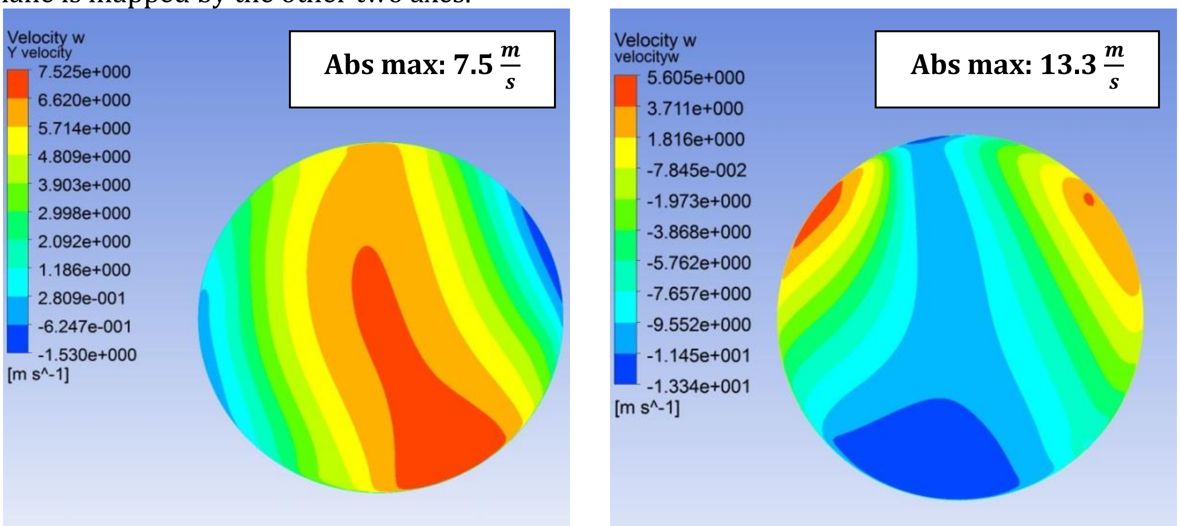

FIGURE 11: TANGENTIAL VELOCITY IN Z-DIRECTION.
LEFT: CEILING CONFIG. /RIGHT: BASEMENT CONFIG

The flow velocity tangential to the surface in w-direction along the z-axis is almost twice as high for the configuration with a double bend as can be seen in Figure 11. This is the first indication that the extra bend indeed introduces extra swirl.

The results shown in Figure 12 lead to the same conclusion. For both the y- and z-direction the velocities are higher in the case of the double bend configuration. This result indicates that the swirl will be higher at the double bend configuration.

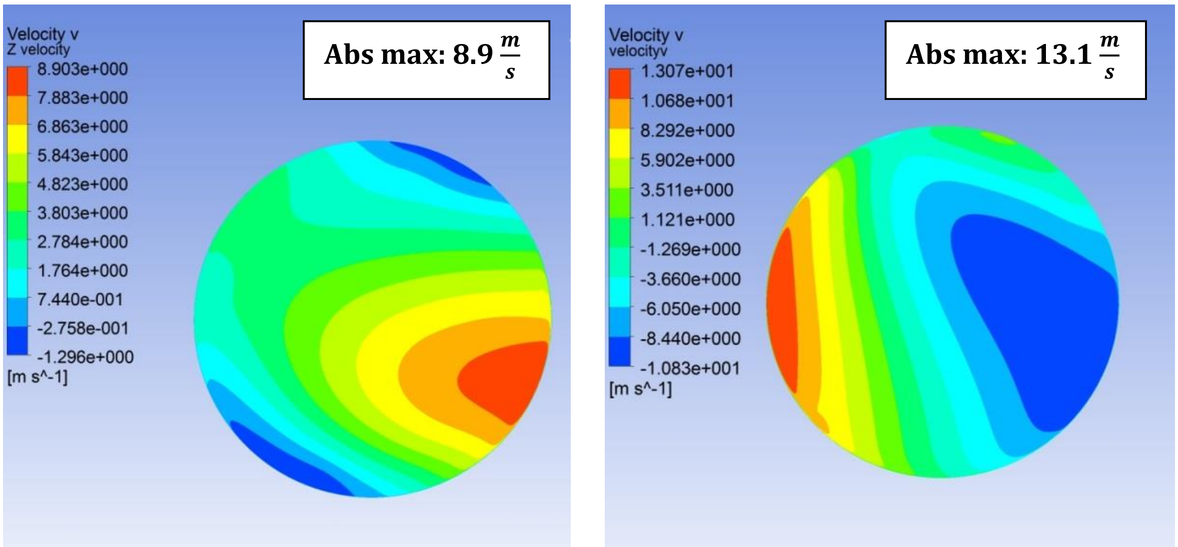

FIGURE 12: TANGENTIAL VELOCITY IN Y-DIRECTION

Taking a step back to the geometry one could argue that orientation of the valve in the pipe can have some influence. In the case of one bend the flow can partially flow straight through the opening of the valve. With two bends the valve is located in such a way that it will probably have more influence on a larger part of the flow. The hypothesis in this case is: A larger part of the flow will tend to flow through the outer radius of the bend, and is more affected compared to the closed part of the valve at the inner radius. Further simulation with rotated valve can be seen in Figure 13.

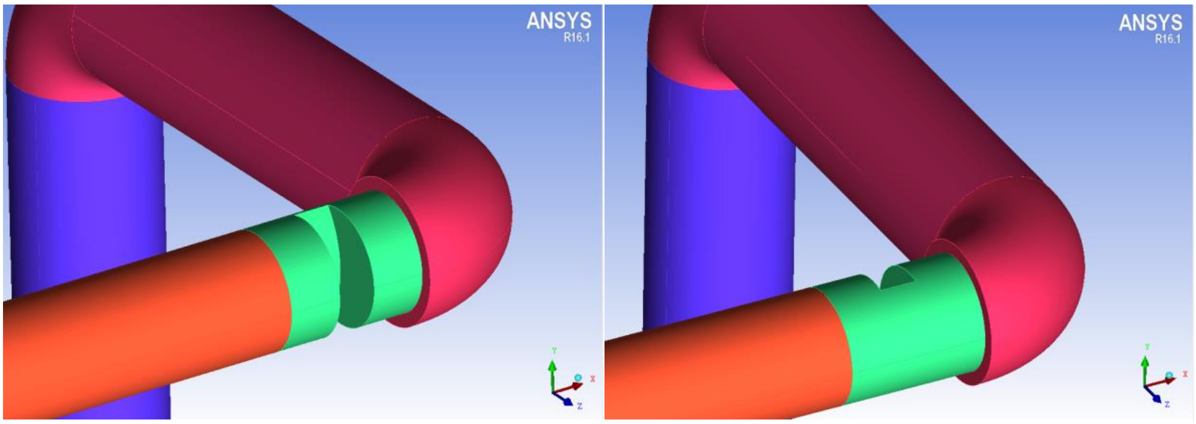

FIGURE 13: VALVE RELATIVE TO CORNER

A simulation with the valve rotated to the inner side, relative to the flow, shows that the speed at the valve is approximately the same at the valve opened for both orientations. Figure 14 shows that the flow accelerates to 145 m/s in the valve. Compared to Figure 9 this is only a difference of 2 m/s.

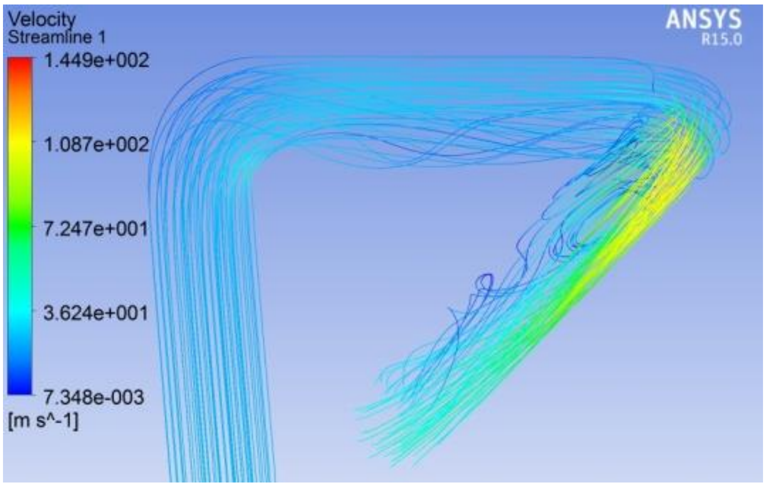

FIGURE 14: STREAMLINES WITH VALVE 180 DEGREES ROTATED

The order of magnitude of the tangential velocities also remains the same, as can be seen in Figure 15. In this figure the absolute magnitude of the flow is still around 13 m/s. This is still twice as high as the flow in the configuration with only one bend.

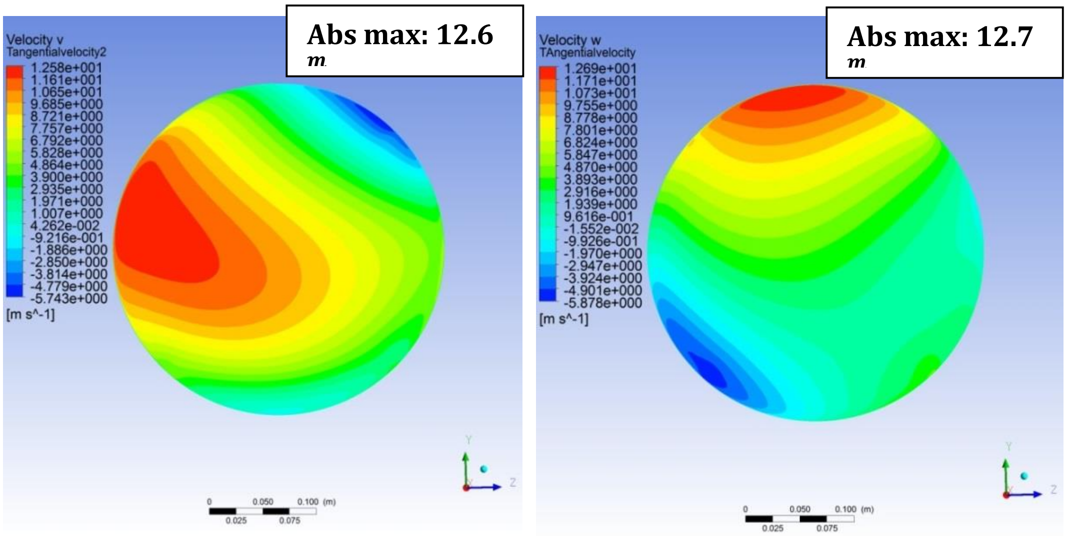

FIGURE 15: TANGENTIAL VELOCITIES
(LEFT: VELOCITY IN Y-DIRECTION; RIGHT: VELOCITY IN Z-DIRECTION)

It can be concluded that with double 90°-bend the swirl is increased and is considerably higher than in case of one bend.

UPDATED LAY-OUT

After performing the simulation there were some new developments regarding the lay-out. Actually, both lay-outs discussed earlier can be combined to have an improved lay-out. A lay-out with one bend and the inlet at the basement of the test facility. The way to achieve this is by positioning the rig on the diagonal of the facility, see Figure 16.

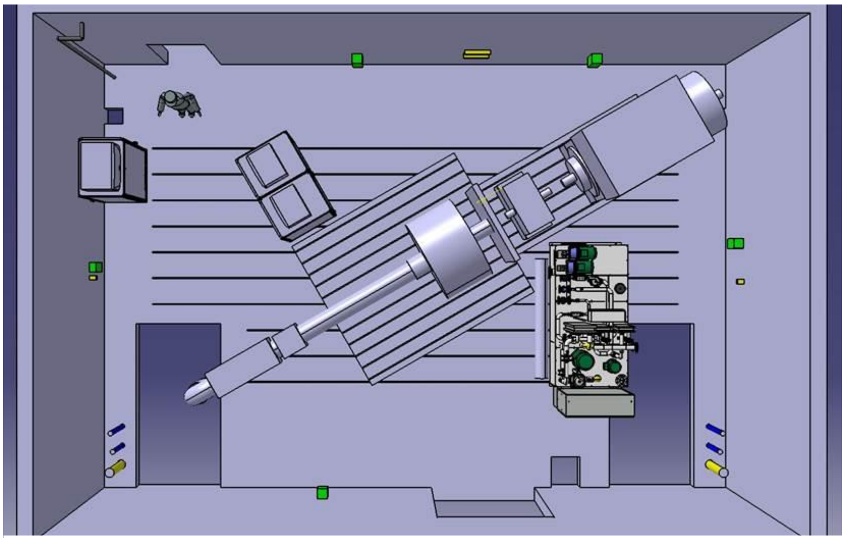

FIGURE 16: TEST FACILITY RE-ARRANGED

FLOW STRAIGHTENER

In any case, the lay-outs described above must guarantee a uniform fully developed flow. Fromt the axial velocity plots, Figure 10 in the previous section, it was already clear that the flow profile is not fully developed. Although the deviation is not that high, uniform flow cannot be guaranteed based on these simulations. For this purpose, a flow straightener, as shown in Figure 17, has been introduced into the piping system to guarantee uniform flow downstream the valve.

Figure 17: Flow straightener (5)

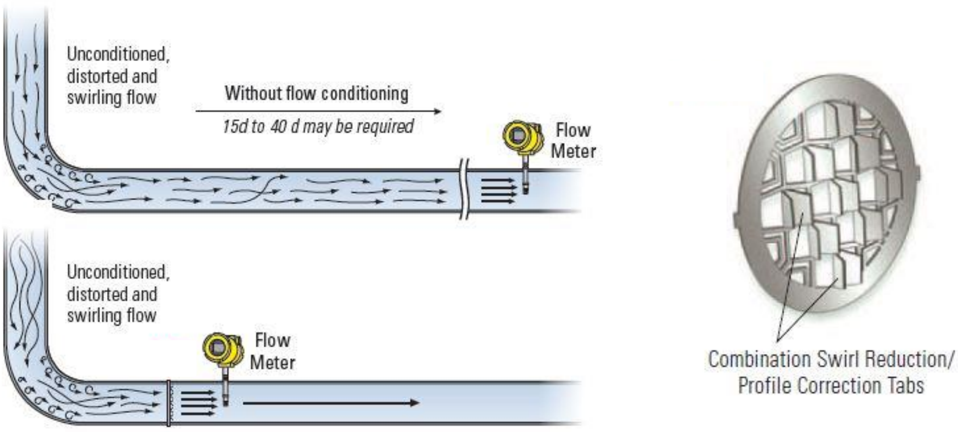

Based on supplier experiments it can be shown that the required length reduces from a minimum of 15 diameters after the valve to only 3-5 diameter lengths. It seems that a flow conditioner does two things:

1. Resistance in the flow will cause the flow profile to be disturbed and to become fully turbulent again which erases the effects of the disturbances. And allows a new flow profile to develop
2. Either tubes or vanes are used to remove any swirl to the flow. Having a look at Figure 17 the vanes are clearly visible.

K.J. Zanker states in an article: “Conditioners obstruct the flow and cause pressure loss. Pressure loss provides the energy to re-distribute the velocity profile. More severe disturbances might require more pressure loss”. (6)

For our case we can deal with pressure drop by the facility so a flow straightener would be a good addition to the system.

PROJECT 2: SECONDARY AIR SYSTEM

The gas flow inside an engine is directed through a complex system of ducts, vents and holes. Primarily the air in an engine is used for propulsion and is therefore called the primary air system. In addition to the primary air flow, there are extra airflows to support the performance of the engine. A combined use of external air and bleed air from the compressor provides the engine with air for cooling, sealing and balancing purposes. As an example the airflow from a CFM56-7B engine is shown (7). It shows the airflow through the bore of the system as coolingstream for the turbine.

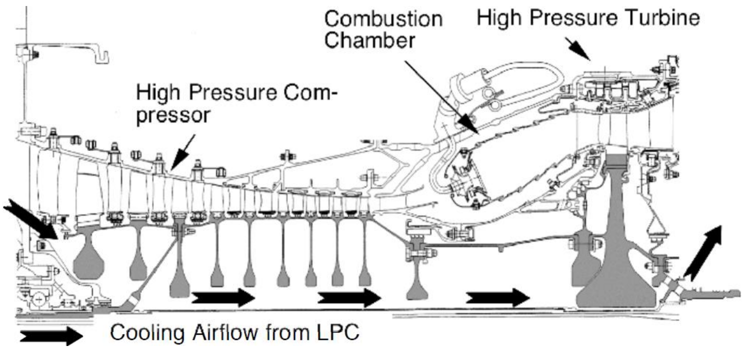

FIGURE 18: AIRFLOW CFM56-7B (7)

TASK DESCRIPTION:

Design the secondary air system for the compressor test-rig and take all components into account by benchmarking the components.

TEST RIG MUNICH

The test rig of Munich is built around a compressor without the presence of the other components of the engine, such as the combustion chamber and turbine. The air which normally would go to the turbine is now directed to an outlet and analyzed. The air has to have the right mass flow, temperature and pressure as if it would be directed to the turbine as a supporting flow with purposes described above.

FIGURE 19: SAS LOCATION IN TEST FACILITY

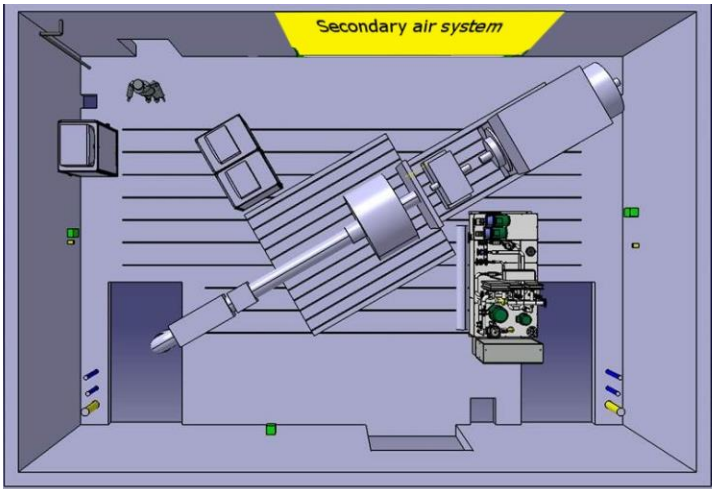

The test rig has to be designed in such a way that all the lines available in a complete engine are also present in the test rig. The required pipes are therefore gathered in one place at the wall where all flowmeters, valves and pipes are installed. The yellow space at the wall in Figure 19 will be used as the mounting area for the secondary air system. An approximate of 3x3 meters is available for mounting the secondary air system (SAS).

It is quite complicated to have a complete overview of all line coming and going to the system. For this report the schematics of the test rig have been simplified to the relevant lines of the secondary air system and can be seen in Figure 20. An explanation of the schematic is given below.

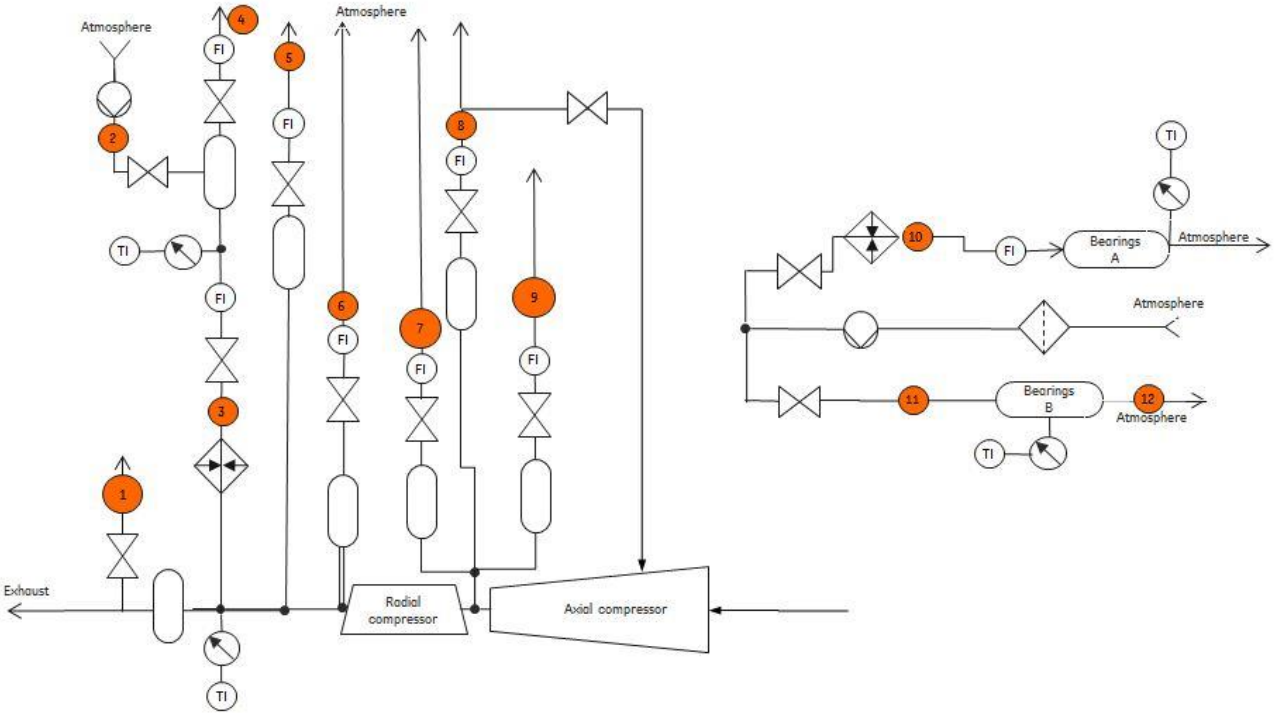

FIGURE 20: SCHEMATIC SAS

- Lines 2, 10 and 11 are supplied from the “atmosphere”, in this case shop air.
- Lines 7, 8 and 9 are bleed lines from the axial compressor at the high pressure side.
- Bleed air from line 8, at higher temperature, is feed back to the compressor.
- Lines 3, 5 and 6 are bleed lines from the radial compressor. Line 3 is routed back to the compressor. The flow is routed through a heat exchanger to cool down the air.
- All air is going to atmospheric conditions again, which is this case means: routed to an outlet pipe.
- A total of 11 flow meters are required in this scheme.
- A total of 12 valves are required in this scheme.
- Line 1 and 12 do not require a flow meter
- Line 12 is just a pipe without devices.

PIPE DESIGN: DIAMETERS

As mentioned in the previous section, the air supply and bleeds from the compressor have to be monitored during the tests in order to analyze the performance of the compressor. A total of 12 different main pipe lines are involved in the secondary air system. For all 12 lines the mass flow, temperature and pressure range are given. These highly changing parameters are the consequence of wide range of tests the compressor has to undergo.

Given the provided data, the required pipe diameters and flow measurement devices can be determined. In this case the speed of the flow may not exceed Mach 0.2 to avoid high pressure losses.

Despite the fact that the Mach number is lower than 0.2, let's consider both compressible and incompressible flow first, as an extra safety step in the analysis. Given a compressible flow and an ideal gas, the pipe diameters can be calculated using:

$$\dot{m} = \frac{AP_t}{\sqrt{T_t R}}\sqrt{\gamma}M(1+\frac{\gamma-1}{2}M^2)^{\frac{\gamma+2}{2-2\gamma}}$$

$$A = \dot{m}\sqrt{T_t R} * \frac{1}{P_t\sqrt{\gamma}M(1+\frac{\gamma-1}{2}M^2)^{\frac{\gamma+2}{2-2\gamma}}}$$

The same can be done if we use a formula for incompressible flow. The maximum of these two equations is chosen as the leading parameter, although the compressibility effect should be minimal. In this case the equation for incompressible flow gives:

$$\dot{m} = U\rho A$$

$$\dot{m} = M * \sqrt{(\gamma R T_t)} * \frac{P_t}{T_t R} * A$$

$$A = \dot{m}\, T_t R * \frac{1}{M * \sqrt{(\gamma R T_t)} * P_t}$$

To calculate the highest speed in the pipes the maximum mass flow, the maximum total temperature and the minimum total pressure are used. Table 1 shows a summary of the diameter calculations for 10 pipes in the system.

Max Mass flow [kg/s]	Max total Temp [^{0}C]	Min Total Pressure [bar]	Required diameter, incompressible flow [m]	Required diameter, compressible flow [m]	Required nominal diameter: DN
0.10	566	1.4	0.043	0.042	50
0.10	260	1.4	0.038	0.037	40
0.23	177	2.8	0.040	0.040	40
0.16	21	2.1	0.035	0.034	40
0.05	316	0.7	0.039	0.038	40
0.03	204	1.4	0.018	0.018	20 (32)
0.19	566	1.4	0.060	0.059	65
0.10	316	0.7	0.055	0.054	65
0.25	316	0.7	0.091	0.089	100
0.08	566	2.1	0.033	0.032	40

TABLE 1: CROSS-SECTIONAL AREA PIPES

The required minimal diameters are now known. The speed, at least in the pipes will not exceed Mach 0.2.

What is missing is the way the pipes are connected to the system. At the high pressure part of the axial compressor air is taken out by lines 7, 8 and 9. For line 7 and 9 the connection is done by a single connection. For line 8 on the other hand this is done by a double connection. The double connection causes a favorable flow behavior in the compressor.

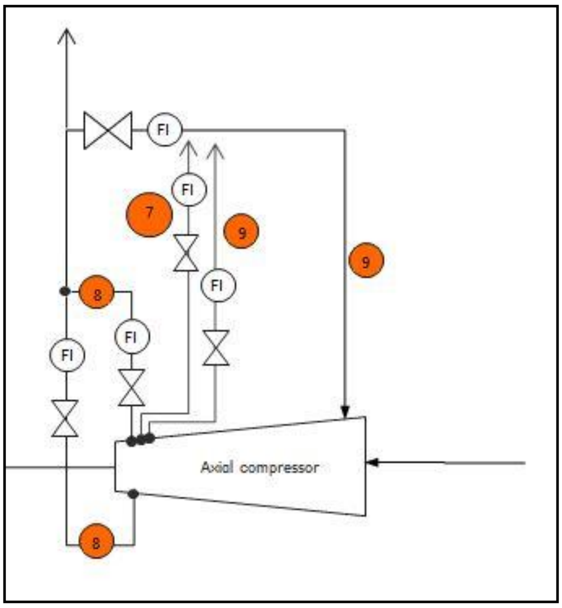

FIGURE 21: LINE SPLIT CONNECTION

The double connections require both a flow meter and a valve. A third valve in line 8 regulates the flow back to the compressor. Figure 21 shows the updated configuration. If one valve is closed all flow must go through the other valve, so these lines become pretty large in the SAS

FLOW METERS

To analyze the flow, proper flow meters have to be installed. The right choice of flow meter is based on a lot of design considerations. The flow meter technologies described below are the ones which are best suitable for our requirements. Other technologies are due to costs, maintenance requirements, safety aspects or accuracy not suitable for this application.

- Turbine flow meters: Internal moving parts, preferred to avoid this risk
- Variable area meters: Not accurate enough and often without digital output
- Coriolis meters: Too expensive while cheaper options are available

Technologies which are applicable:

- Differential pressure flow meter
- Thermal flow meter
- Vortex flow meter

Differential pressure flow meters:

Differential pressure flowmeters use Bernoulli's principle to measure the flow of fluid in a pipe. Differential pressure flowmeters introduce a constriction in the pipe that creates a pressure drop across the flowmeter. When the flow increases, more pressure drop is created. The pressure is measured upstream and downstream of the flowmeter and is directed to the transmitter that measures the differential pressure to determine the fluid flow. This technology is a widely used technology because it is relatively cheap and easy to install (8).

Thermal flow meters:
Thermal flowmeters use the thermal properties of the fluid to measure the flow of a fluid flowing in a pipe or duct. In a typical thermal flowmeter, a measured amount of heat is applied to the heater of the sensor. Some of this heat is lost to the flowing fluid. As flow increases, more heat is lost. The amount of heat lost is sensed using temperature measurement(s) in the sensor. The transmitter uses the heat input and temperature measurements to determine fluid flow. Most thermal flowmeters are used to measure gas flows. A big advantage is the direct measurement of mass flow (9).

Vortex flow meter:
The measuring principle is based on the development of a Karman vortex shedding sheet in the wake of a body built into the pipeline. A blunt body in the flow generates a so-called "Karman vortex street" with alternating pressure conditions whose frequency is proportional to the flow velocity.

	Thermal meter	Differential pressure meter	Vortex meter
Accuracy	+- 1% Full scale	+- 1-2% Full scale	+- 0.5-1% Full Scale
Temperature limit [K]	650	Typical around 1000	Typical around 1000
Turndown ratio	100:1	5:1	30:1 (with minimum velocity required)
Required upstream pipe length	15D	15D	15D
Price	$$	$	$$-$$$

TABLE 2: DATASHEET FLOW METER

In Table 2, a basic comparison between the three types of flow meters is made. The thermal flow meter has relative high accuracy but is limited on the temperature. The turndown ratio for differential pressure meter is very limited but is relatively cheap compared to the others. Vortex flow meters have high accuracy and can handle higher temperature but require Re>10000 since no or little vortex shedding is created when the flow velocity is low.

From a company point of view, it is preferred to have as little as possible different technologies, since it would increase the amount of suppliers. Since the vortex devices cannot handle low flow velocities, we choose to continue only with the differential pressure and thermal devices.

ACCURACY OF A FLOW METER

In general, two different ways of defining the accuracy are used. The accuracy based on the full scale flow and the accuracy as percentage of the measured flow. Most suppliers deliver a product specification with a combination of these accuracies. The accuracy of reading is just the error of actual reading. More significant at low flow rates can be the FS percentage error. The local error as function of the percentage of full scale flow, with an accuracy of 1% at full scale, is given in Figure 22. Let's say that the flow rate is 0.1 kg/s, an error of 1% full scale would mean an error of 0.001 kg/s. At 10% of the full scale flow, so 0.01 kg/s, the error has increased to 10%.

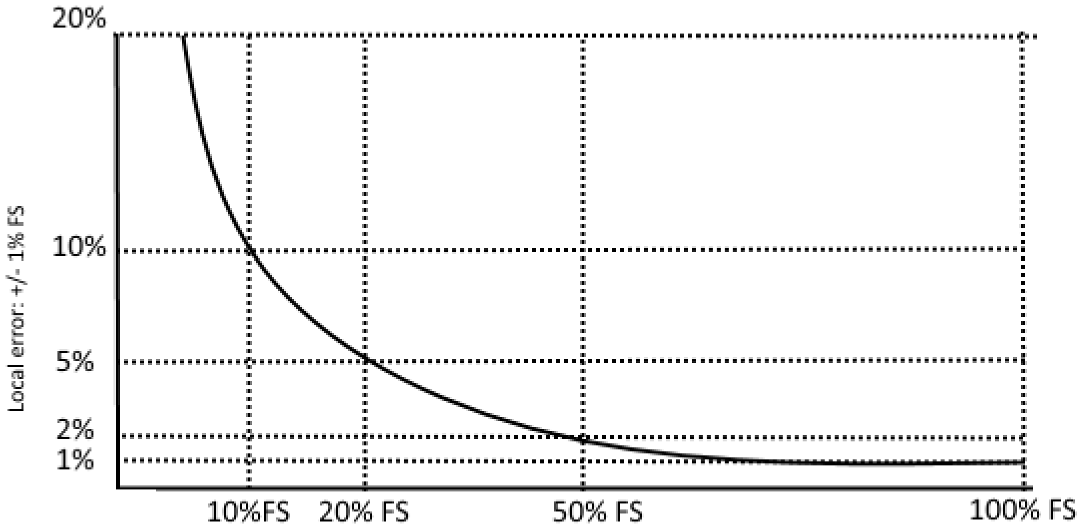

FIGURE 22: LOCAL ERROR AS FUNCTION OF PERCENTAGE OF FULL SCALE FLOW

TURNDOWN RATIO

The turndown for a differential pressure device, in this case the orifice plate, is low compared to the thermal flow measurement devices. The turndown ratio tells you till what percentage of the full scale flow the calibrated accuracy can be guaranteed. The turndown ratio is defined as:

$$\boldsymbol{Turndown} = \frac{Full\ scale\ flow}{Minimum\ flow}$$

Where the volume flow can be calculated using

$$\dot{V} = \frac{\dot{m}TR}{P}$$

For an orifice plate this is typical 5:1, so this means if the flow is below 20% of the maximum flow, the accuracy cannot be guaranteed. The turndown ratios for the lines in the secondary air system are determined using the parameters shown in Table 3. The calculations have been done using the extreme parameters, so the ratios are also the extremes of the flow.

Mass flow range [kg/s]		Temp range [^{0}C]		Total Pressure range [bar]		Turndown ratio (based on volume flow)
0.005	0.10	204	593	1.4	11.0	35
0.005	0.10	66	260	1.4	10.3	236
0.010	0.23	21	177	2.8	4.1	57
0.005	0.16	21	21	2.1	11.4	193
0.003	0.05	66	316	0.7	6.6	25
0.004	0.02	21	204	1.4	2.8	20
0.023	0.18	177	566	1.4	11.7	15
0.068	0.09	66	316	0.7	6.6	2
<0.005	0.25	66	316	0.7	6.6	4
0.068	0.08	182	566	2.1	17.2	2

TABLE 3: TURNDOWN RATIOS

Based on the calculation above, looking at the temperature limits and costs we now are able to choose a device which suits our requirements. The selection is shown in Table 4, where the colored cells show if it is applicable (green), maybe applicable (orange) or not applicable (red). A choice can be made for 8 lines directly, as shown in the right column.

Turndown ratio (based on volume flow)	Differential pressure: Orifice	Thermal flow meter	Choice
35	Turndown	Temperature	T.B.D.
236	Turndown		Thermal
57	Turndown		T.B.D.
193	Turndown		Thermal
25	Turndown		T.B.D.
20	Turndown		T.B.D.
15		Temperature	Orifice
2			Orifice
4			Orifice
4			Orifice
4			Orifice
2		Temperature	Orifice

TABLE 4: METER SELECTION

The turndown for four lines is somewhat high to directly choose an orifice as the device to use. Since it turns out that these turndowns are based on the very high limits of the flow we choose to use orifice plates despite the inaccuracy at very low volume flows. The very lower limit of the flow will not occur in the critical region of the flow where the measurements need to take place.

VALVES

To control the mass flow valves are used in every line. Since there is a reliable supplier which chooses the right valves if we supply them with the right parameters there is no real choice to be made on the supplier. Figure 23 shows the valve used for our application.

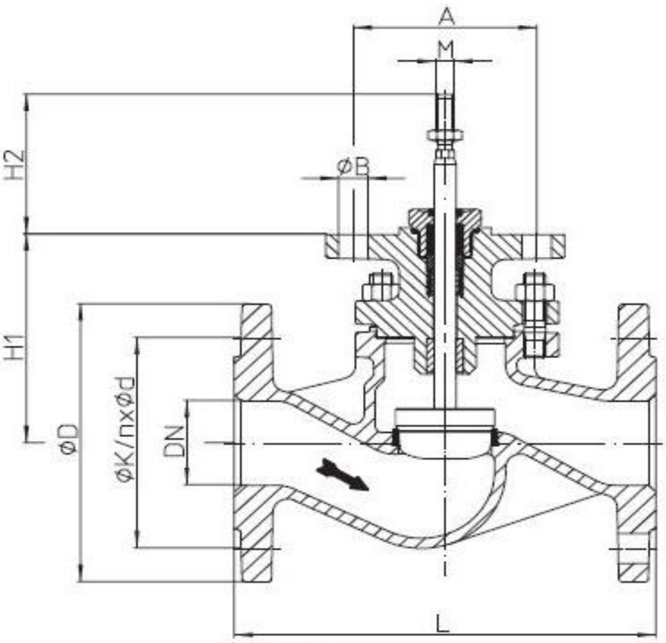

FIGURE 23: STEVI 440 VALVE (10)

The interesting part for now is the required space of the valves, since the valves determine the width of the lines. The dimensions of the valves can be seen in Figure 24. Especially for the larger valves the dimensions highly determine the total dimensions of the SAS system.

DN			15	20	25	32	40	50	65	80	100	125	150
Abmessungen													
M	Fig. 440	(mm)	M10						M14 x 1,5			M16 x 1,5	
	Fig. 441	(mm)	M12									M16	
H1	Fig. 440	(mm)	103		111		118	124	137	152	171	210	270
	Fig. 441	(mm)	288		296		287	289	373	385	401	565	596
H2	Fig. 440 / Fig. 441	(mm)	83										
A	Fig. 440 / Fig. 441	(mm)	100										
n x ØB	Fig. 440 / Fig. 441	(mm)	2 x 16										
Baulänge FTF Grundreihe 1 nach DIN EN 558													
L		(mm)	130	150	160	180	200	230	290	310	350	400	480
Flansche nach DIN EN 1092-1/-2			Flanschbohrungen/-dickentoleranzen nach DIN 2533/2544/2545										
ØD	PN16	(mm)	95	105	115	140	150	165	185	200	220	250	285
	PN25	(mm)									235	270	300
	PN40	(mm)											

FIGURE 24: STEVI VALVE DIMENSIONS (10)

HEAT EXCHANGER

One of the supply lines is actually a feedback from the high pressure part of the compressor. Bleed air from the high pressure part of the compressor makes a loop back to a latter part of the compressor the back wall of the impeller. There is a temperature limit to the back wall so a heat exchanger is required to cool the air.

The air has to be cooled down in order to have the required temperatures at the impeller back wall. A heat exchanger with water as cooling medium is designed.

There is a high variety of heat exchanger available on the market, but for a simple analysis two types of heat exchanger can be distinguished. The tube-shell heat exchanger and the plate heat exchanger. In general, a heat exchanger based on the tube-shell principle is:

1. Less expensive as compared to Plate type coolers
2. Can be used in systems with higher operating temperatures and pressures
3. Pressure drop across a tube cooler is less

On the other hand:

1. Heat transfer efficiency is less compared to plate type cooler
2. Requires more space in comparison to plate coolers.
3. Capacity of tube cooler cannot be increased.

Since we have to deal with high temperatures the plate heat exchanger will not work properly, this means the tube-shell heat exchanger is the best choice for our case. The best performance is reached while having a counter flow in the heat exchanger, as shown in Figure 25.

The amount of heat to be dissipated is given using:

$$\dot{Q} = \dot{m} * c_p * (T_{b1} - T_{b2})$$

$$\dot{Q} = 0.0907 * 1029 * 200 \approx 18kW$$

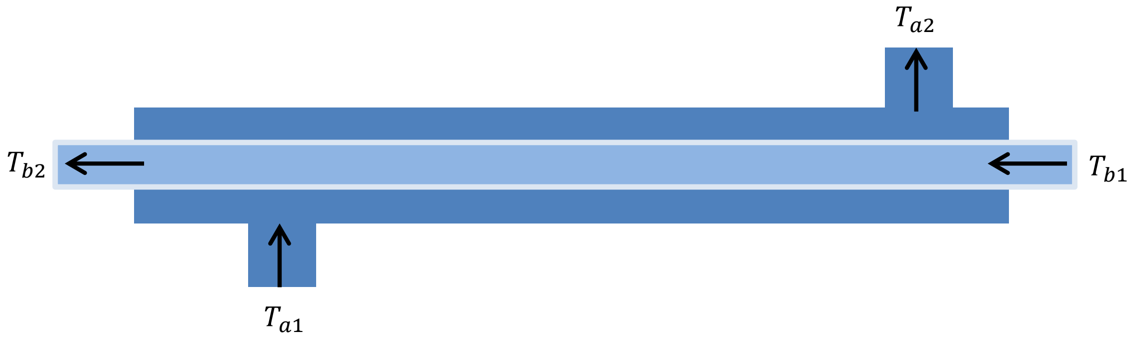

FIGURE 25: COUNTERFLOW HEAT EXCHAGNER

After requesting a preliminary design at the supplier we can have a look at the approximated dimensions. It turns out that a heat exchanger for this purpose is not that large at all. Based on the supplier data the heat exchanger would be approximately have the dimensions as given in Figure 26.

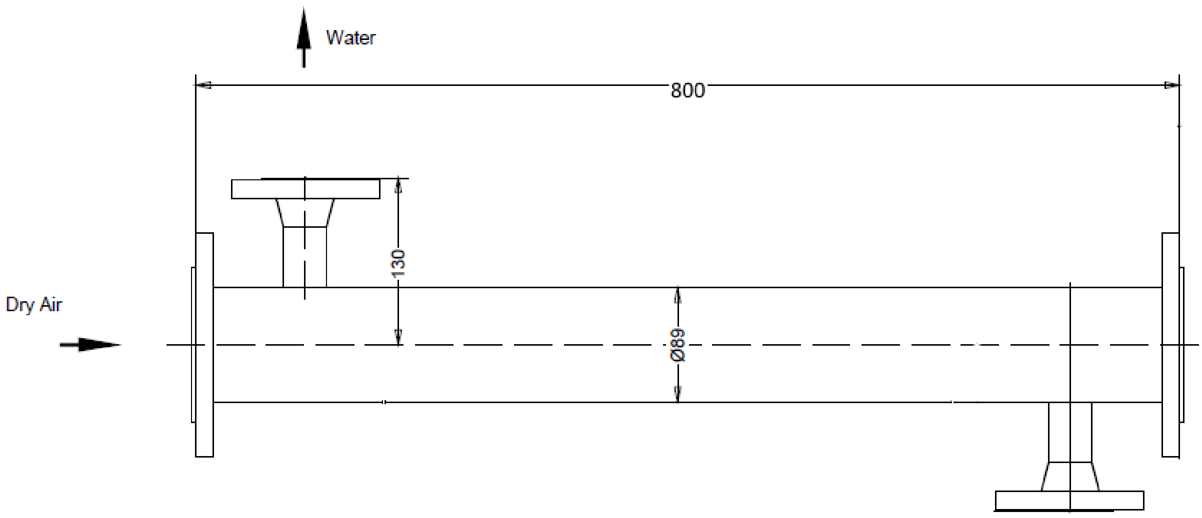

FIGURE 26: HEAT EXCHANGER DIMENSIONS

For the design of the SAS these dimensions are now sufficient to be able to make the dimensional drawings. No further work is done on the heat exchanger part because not all parameters are fixed yet. Detailing the heat exchanger would be something to do when the design of the SAS is at a more detailed phase of the project.

SAS DESIGN

Now all important components have been taken into account, the first drawings can be made to estimate the required space. The design sketch can be seen in Figure 27. All vertical pipes are mounted within the yellow marked place in the facility

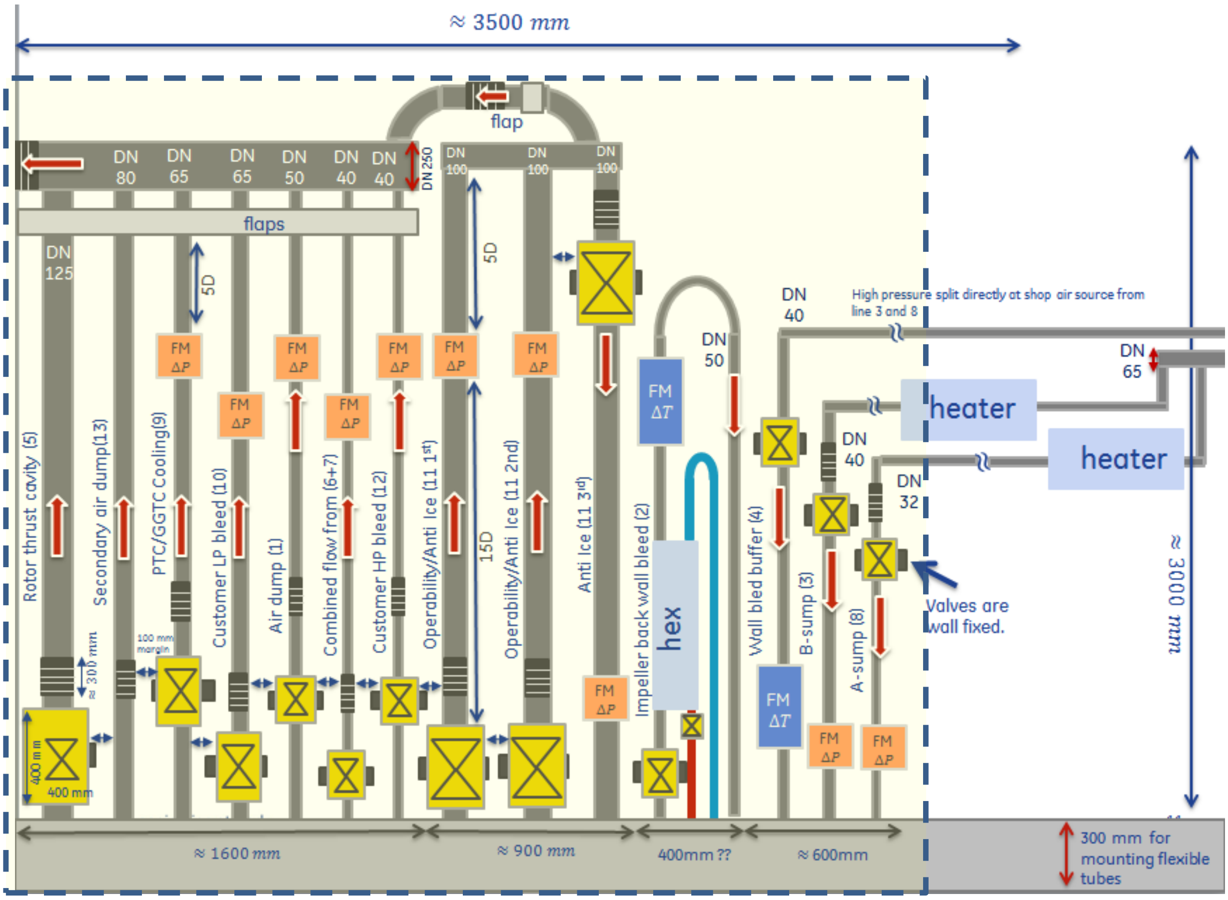

FIGURE 27: SAS

Let's have a closer look at the configuration:

- The pipes coming from the compressor are located at the left side of the SAS since the outlet to the ambient environment is at the left top corner.
- The incoming pipes to the compressor are located at the right hand side since the shop air source is located at the right side.
- The inlet from the shop air is split into a high pressure line and two lines which require low pressure. The split is done directly at the shop air source due to safety reasons.
- Two of the shop air lines require a heater since the shop air is only available at ambient temperature and need to be heated to 400 degrees Fahrenheit
- The valves are mounted at the wall since they have a high mass compared to the other components
- The flow meters are mounted downstream of the valves. The pressure at the pressure taps in the orifice meters will be approximate ambient and allows more accurate measurements.

- Compensators are installed in the high temperature lines. Below the valves the pipes can handle thermal expansion. Above the valves extra compensators are required.

PRESSURE LOSSES

Given the design in previous section, a basic guess of the pressure losses can be made. The pressure losses will be large at the orifice plates and valves. Since, the way of calculation the pressure losses over these devices, is very extensive and different for the different parts we have a look at the general pressure losses. For an incompressible steady flow and neglecting the effects of gravity the total energy of the system can be described as:

$$P_1 + \rho \frac{U_1^2}{2} = P_2 + \rho \frac{U_2^2}{2} + P_{losses}$$

The losses can be divided into two parts:

$$P_{losses} = P_{major\_loss} + P_{minor\_loss}$$

In contradiction to the names, minor loss can be significant compared to major loss. When a valve is almost closed these losses become very large. For an open valve the minor loss can often be neglected.

The major losses occur due to friction as is for a fully developed, steady, incompressible flow described as:

$$P\_major = \left(\frac{\rho U^2}{2}\right)\left(f \frac{L}{d}\right)$$

Where “f ” is the friction factor. The friction factor depends on the Reynolds number and the roughness of the surface area. The equation is also known as the D’Arcy -Weiβbach formula. The minor losses also relate to the dynamic pressure of the flow and are given by

$$P\_minor = \left(\frac{\rho U^2}{2}\right)(\zeta)$$

The minor loss coefficient ζ, mainly depends on the geometry of the object and the Reynolds number.

As explained earlier the pressure losses depend on a lot of different parameters. Especially the coefficient which also depends on the Reynolds number could even be larger than the velocity term in the equations. But since we don’t know these right now we assume the effect of these parameters to be less than the influence of the volume flow on the pressure losses.

Pressure losses increase when diameter decreases, length increases or the roughness of the surface increases, but the most interesting part is the velocity.

$$U = \frac{\dot{V}}{A} = \frac{4\dot{m}}{\rho \pi d^2}$$

This means that for small diameters and high mass flows the pressure losses can be considerably high.

Having a look at the lines in the SAS design of Figure 27 and the data from Table 1 we can see that the pressure losses will be high in line 9. It has one of the highest mass flows, highest temperatures, lowest pressure and relative small diameter.

Calculating the pressure losses using software specialized in pressure losses, we can see that the pressure losses over the main part of line 9 are approximately 0.25 Bar. For further details one can see the calculation sheet as attachment to this report.

CONCLUSION

Of course the design of the SAS is not finished but the main components have been analyzed and a solid basic lay-out has been established. The next step of the design would be ordering the right components based on the requested quotes after all data is fixed and the input parameters do not change anymore.

INTERNSHIP: ACHIEVED GOALS

During my internship I have helped on a lot of small topics where two main projects can be distinguished; CFD simulations for the inlet and the design of the secondary air system. Being able to do so many different things has given me a good insight in a big project as this. I managed to improve my skills on CAD, CFD and meshing and was able to learn some practical things like contacting suppliers, requesting and gaining knowledge on system components I never encountered before.

BIBLIOGRAPHY

1. **Benvie, Matt.** The biggest win. *GE Reports.* [Online] November 16, 2015. [Cited: March 15, 2016.]

2. **FCI.** Best Engineering Practices. *fluidcomponents.* [Online] [Cited: 04 14, 2016.] http://www.fluidcomponents.com/Industrial/Library/manuals/General/Best%20Practices%20Engineering%20GuideFINAL.pdf.

3. SST k-omega model. *CFD-online.* [Online] [Cited: 05 30, 2016.] http://www.cfd-online.com/Wiki/SST_k-omega_model.

4. **ANSYS SAS IP, inc.** *Introduction to ANSYS ICEM CFD.* 2013.

5. **Vortab.** Brochure. *Vortab.com.* [Online] [Cited: March 30, 2016.] http://www.vortab.com/pdfs/Vortab-Brochure-RevF.pdf.

6. *Devices used to pre-condition the gas flow profile prior to measurement.* **K.J.Zanker.** Houston Texas USA : Letton-Hall Group.

7. **CFM.** *CFM56-7B Engine Systems.* Medlun-Montereau Cedex, France : CFM International, 2000.

8. **UFM.** Differential pressure flowmeter technology. *flowmeters.* [Online] [Cited: May 25, 2016.] http://www.flowmeters.com/differential-pressure-technology.

9. —. Thermal Flowmeter Technology. *Flowmeters.* [Online] UFM. [Cited: 25th May, 2016.] http://www.flowmeters.com/thermal-technology.

10. **Armaturen, ARI.** Stevi Valves. *Ari-armaturen.* [Online] [Cited: May 25th, 2016.] http://www.ari-armaturen.com/_appl/files_tb/files/440001-2.pdf.

ATTACHMENT 1: PRESSURE LOSSES

Projekt: Line 9						
		1	2	3	4	5
1. Fördermedium						
Fördermedium		Luft	Luft	Luft	Luft	Luft
Aggreg.Zustand		gasförmig	gasförmig	gasförmig	gasförmig	gasförmig
Volumenstrom	m3/h	991,880597	991,880597	1009,969605	1100,264901	1134,061433
Massenstrom	kg/h	664,56	664,56	664,56	664,56	664,56
Volumenstrom abzw.Rohr	m3/h					
Dichte	kg/m3	0,67	0,67	0,658	0,604	0,586
Dyn.Viskos.	10-6 kg/ms	35,065	35,065	35,064	35,064	35,063
Kin.Viskos.	10-6 m2/s	52,3358209	52,3358209	53,2887538	58,05298013	59,83447099
2. Zusätzliche Daten für Gase						
Eintritts-Druck (abs.)	bar	1,4	1,385	1,375	1,262	1,225
Eintritts-Temperatur	°C	454	454	454	454	454
Austritts-Temperatur	°C	454	454	454	454	454
Normvolumenstrom	Nm3/h	514,8112329	509,2953983	514,8391753	514,7747042	515,0308623
3. Rohrleitungselement						
Rohrbezeichnung			bend at wall	Valve	Valve to FM	Orifice
Rohrleitungselement		Kreisrohr	Kreiskrümmer	Geradsitzventil	Kreisrohr	Lochscheibe
Anzahl		1	1	1	1	1
Elementabmessungen	SI	Rohrdurchmesser D: 65,00 mm	Rohrdurchmesser D: 65,00 mm	Rohrdurchmesser D: 65,00 mm	Rohrdurchmesser D: 65,00 mm	Rohrdurchmesser D1: 65,00 mm
		Rohrlänge L: 2,00 m	Radius R: 100,00 mm		Rohrlänge L: 1,50 m	Durchmesser D2: 50,00 mm
			Winkel w: 90,00 Grad			Länge L: 6,00 mm
4. Berechnungsergebnis						
Strömungsgeschw.	m/s	83,0310059	83,0310059	84,54524917	92,10393039	94,93306136
Reynolds-Zahl		103122,7808	103122,7808	103125,7217	103125,7217	103128,6629
Strömungsgeschw.2	m/s					160,4368737
Reynolds-Zahl 2						134067,2618
Strömungsform		turbulent	turbulent	turbulent	turbulent	turbulent
Rohrrauhigkeit	mm	0,05	0,05		0,05	
Rohrreibungszahl		0,021281976	0,021281976		0,021281911	
Zeta-Wert		0,654830017	0,394244128	5,577622276	0,491121013	1,927458527
Zeta-Wert abzw.Rohr						
Druckv. abzw.Rohr	mbar					
Druckverlust	mbar	15,20613925	9,135352139	138,1019757	12,6454154	52,00014643
Druckverlust	bar	0,015206139	0,009135352	0,138101976	0,012645415	0,052000146
Summe Druckverlust	bar	0,015206139	0,024341491	0,162443467	0,175088882	0,227089029

Projekt:	Line 6+7					
		1	2	3	4	5
1. Fördermedium						
Fördermedium		Luft	Luft	Luft	Luft	Luft
Aggreg.Zustand		gasförmig	gasförmig	gasförmig	gasförmig	gasförmig
Volumenstrom	m3/h	147,3085339	147,956044	148,2819383	151,7925592	152,1355932
Massenstrom	kg/h	134,64	134,64	134,64	134,64	134,64
Volumenstrom abzw.Rohr	m3/h					
Dichte	kg/m3	0,914	0,91	0,908	0,887	0,885
Dyn.Viskos.	10-6 kg/ms	28,348	28,348	28,348	28,347	28,347
Kin.Viskos.	10-6 m2/s	31,01531729	31,15164835	31,22026432	31,95828636	32,03050847
2. Zusätzliche Daten für Gase						
Eintritts-Druck (abs.)	bar	1,4	1,394	1,391	1,359	1,355
Eintritts-Temperatur	°C	260	260	260	260	260
Austritts-Temperatur	°C	260	260	260	260	260
Normvolumenstrom	Nm3/h	104,2776227	104,2871174	104,2918961	104,3049979	104,2330165
3. Rohrleitungselement						
Rohrbezeichnung		compressor top wall	Lower bend at wall	Valve	Valve to FM	
Rohrleitungselement		Kreisrohr	Kreiskrümmer	Geradsitzventil	Kreisrohr	Lochscheibe
Anzahl		1	1	1	1	1
Elementabmessungen	SI	Rohrdurchmesser D: 40,00 mm	Rohrdurchmesser D: 40,00 mm	Rohrdurchmesser D: 40,00 mm	Rohrdurchmesser D: 40,00 mm	Rohrdurchmesser D1: 40,00 mm
		Rohrlänge L: 2,00 m	Radius R: 100,00 mm		Rohrlänge L: 1,50 m	Durchmesser D2: 25,00 mm
			Winkel w: 90,00 Grad			Länge L: 6,00 mm
4. Berechnungsergebnis						
Strömungsgeschw.	m/s	32,56233518	32,70546633	32,7775048	33,55352239	33,62934956
Reynolds-Zahl		41995,1663	41995,1663	41995,1663	41996,64777	41996,64777
Strömungsgeschw.2	m/s					86,09113487
Reynolds-Zahl 2						67194,63643
Strömungsform		turbulent	turbulent	turbulent	turbulent	turbulent
Rohrrauhigkeit	mm	0,05	0,05		0,05	
Rohrreibungszahl		0,025239564	0,025239564		0,025239443	
Zeta-Wert		1,261978183	0,468765916	6,575718396	0,946479102	7,598930163
Zeta-Wert abzw.Rohr						
Druckv. abzw.Rohr	mbar					
Druckverlust	mbar	6,128451142	2,283305053	32,45239254	4,734106098	38,57707591
Druckverlust	bar	0,006128451	0,002283305	0,032452393	0,004734106	0,038577076
Summe Druckverlust	bar	0,006128451	0,008411756	0,040864149	0,045598255	0,084175331